

Article

Cooling Performance of Fresh and Aged Automatic Transmission Fluids for Hybrid Electric Vehicles

Noelia Rivera ¹, José Luis Viesca ^{2,3} , Alberto García ² , Jose I. Prado ⁴ , Luis Lugo ⁴ 
and Antolin Hernández Battez ^{2,3,*} 

- ¹ Department of Marine Science and Technology, University of Oviedo, Blasco de Garay, s/n, 33203 Gijón, Spain
² Department of Construction and Manufacturing Engineering, University of Oviedo, Pedro Puig Adam, s/n, 33203 Gijón, Spain
³ Department of Design and Engineering, Bournemouth University, Poole BH12 5BB, UK
⁴ CINBIO, Universidade de Vigo, Grupo GAME, Departamento de Física Aplicada, 36310 Vigo, Spain
* Correspondence: aehernandez@uniovi.es; Tel.: +34-985-18-2669

Abstract: The cooling performance of automatic transmission fluids (ATFs) plays an important role in hybrid electrical vehicles, in which the electric motor (EM) is placed inside the transmission housing due to their mission of cooling the EM. The cooling performance of the ATFs depends on their thermophysical properties, but these properties change with the oxidation of the ATFs. This work studies the influence of the oxidation of three ATFs (A, B, C) on their thermophysical properties, as well as on some figures-of-merit (FOMs) which are relevant for evaluating the cooling performance. The results indicated that the influence of the molecular structure on thermal conductivity and heat capacity is stronger than on density and viscosity, whereas the molecular structure hardly affects the FOMs of the fresh ATFs; ATFs B and C, formulated with base oils from API Group III, indicated better cooling performance than ATF A which was formulated with base oils from API Group I; the sensitivity to temperature of the variation with oxidation of the studied properties, including the FOMs, was almost null, except for ATF A; therefore, FOMs should be used to compare the cooling performance of ATFs for electric drivetrains instead of a single property, such as thermal conductivity.

Keywords: automatic transmission fluids; hybrid electric vehicles; thermal conductivity; heat capacity; viscosity; density



Citation: Rivera, N.; Viesca, J.L.; García, A.; Prado, J.I.; Lugo, L.; Battez, A.H. Cooling Performance of Fresh and Aged Automatic Transmission Fluids for Hybrid Electric Vehicles. *Appl. Sci.* **2022**, *12*, 8911. <https://doi.org/10.3390/app12178911>

Academic Editor: Ramin Rahmani

Received: 31 July 2022

Accepted: 2 September 2022

Published: 5 September 2022

Publisher's Note: MDPI stays neutral with regard to jurisdictional claims in published maps and institutional affiliations.



Copyright: © 2022 by the authors. Licensee MDPI, Basel, Switzerland. This article is an open access article distributed under the terms and conditions of the Creative Commons Attribution (CC BY) license (<https://creativecommons.org/licenses/by/4.0/>).

1. Introduction

The use of electric vehicles (EVs) is one of the main solutions for reducing global warming and the increasing requirements for greenhouse gases reduction. Thus, most light vehicles will be driven by electric or hybrid motor systems by 2029 [1]. The forecast for hybrid electric vehicle (HEV) production in the coming years is the highest among the different classes of EVs. In the HEVs, the electric motors (EMs) can be in different positions. When the EM is incorporated inside the transmission or axle, the lubricant is in contact with the EM and should therefore fulfil specific requirements. An example of this configuration is the Multistage Hybrid System (Figure 1) developed by Toyota and installed in vehicles since 2017. Some of these requirements are compatibility with the structural materials used in the EM, electrical compatibility, prevention of copper corrosion of the electrical components, magnetic compatibility, and the avoidance of foaming and aeration due to the high speeds ($\geq 20,000$ rpm) [2]. Additionally, the lubricants used in transmissions and axles in such HEV configurations must assure the cooling of the EM, so their heat transfer behavior plays an important role [3–5].

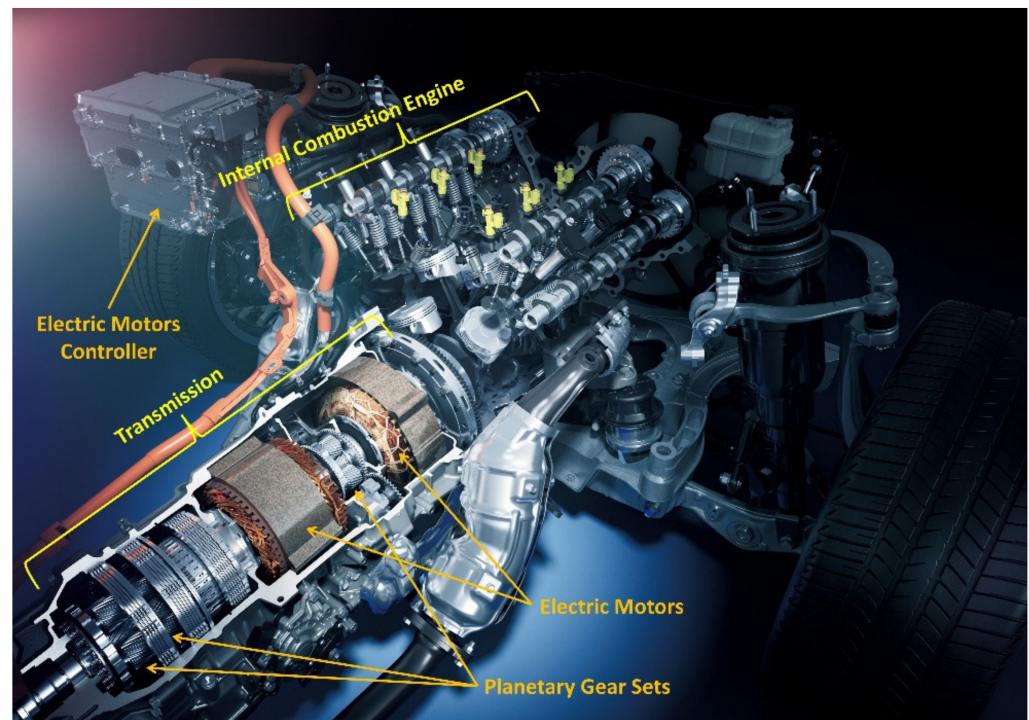


Figure 1. Toyota Multistage Hybrid System [6]. Hybrid powertrain for a passenger car composed of an internal combustion engine and an electrified transmission with two electric motors inside the planetary gearbox.

There are different methods for cooling EMs: air cooling, water cooling and oil cooling, but the miniaturization and required high performance for EVs led to the use of the oil-cooling method as the best option [7]. Heat conduction enhancement and hybrid thermal management have also been studied as options for cooling EMs [8]. Huang et al. [9,10] compared indirect and direct oil cooling methods, direct ones being superior. They reduced the average temperature rise of the coolant at the inlet by a factor of between 1.5 and 3 and improved the heat transfer performance. The best cooling results were obtained with a direct oil method, reducing the maximum temperature to 403.6 K (130.45 °C). Alexandrova et al. [11] reported maximum temperatures of 420.15 K (147 °C) and 377.15 K (104 °C) for the rotor and the stator, respectively, when general oil cooling was used. On the other hand, Lim et al. [12] reported temperatures of 380.15 K (107 °C) and 362.95 K (89.8 °C) for those components, respectively, when lubricating the coil and housing with the oil spray cooling method. Lower temperatures, 350.15 K (77 °C) for the rotor and 333.15 K (60 °C) for the stator, were reached using a hybrid cooling method (hollow shaft oil cooling + housing cooling).

Automatic transmission fluids (ATFs) should ideally maintain the materials, magnetic, and electrical compatibilities, the copper corrosion protection, and avoid foaming and aeration over time, and thus achieve the desired “fill-for-life” status. For this reason, studying how the heat transfer characteristics change due to the aging of the ATFs and the influence of their formulation on these characteristics is very important. Today EV and HEV designs are also using conventional ATFs for ICEV (internal combustion engine vehicles) with acceptable performance, but this solution is not optimized for the performance of the EV and the HEV [3]. Effective cooling of the EM allows for a higher vehicle efficiency and therefore the heat dissipation requirement of the lubricant is increased. This demands higher thermal stability and improved heat transfer performances of the ATFs used in HEVs and EVs than of their conventional counterparts. Conversely, the use of low-viscosity lubricants in engines and transmissions is a current trend, intended to reduce churning and drag losses. However, these low-viscosity lubricants must also protect the hardware and

therefore the lubricant chemistry must be improved by using new base oils and additives at different concentrations.

As for any other heat transfer fluid (HTF) or coolant, the thermophysical properties (density, viscosity, heat capacity, and thermal conductivity) of the ATFs are necessary to determine its heat transfer performance. The ATFs must demonstrate high heat transfer performance and low pumping power, low fluid volume, and low heat losses or low temperature drop [13]. Thus, fluids with high densities, thermal conductivities, and heat capacities, in addition to low viscosities, are preferred when selecting ATFs. Nevertheless, materials usually demonstrate good values for some properties but poor ones for others, so finding criteria for comparing and selecting possible candidate fluids is mandatory. In this case, it is useful to use a figure of merit (FOM), which is a numerical quantity based on one or more characteristics of a system or device and represents a measure of efficiency or effectiveness. The Mouromtseff number (Mo) is a dimensionless FOM that can be used to quantify the heat transfer performance of the ATFs [1,14] and this is defined as:

$$\text{Mo} = \rho^a \cdot k^b \cdot C_p^c \cdot \mu^d \quad (1)$$

where a , b , c , and d are constants which are dependent on the heat transfer mode and represent the sensitivity to the different thermophysical properties [15]. The Mouromtseff number for forced convection is calculated as:

$$\text{Mo} = \frac{\rho^{0.8} \cdot k^{0.6} \cdot C_p^{0.4}}{\mu^{0.4}} \quad (2)$$

In addition, some other FOMs (Equations (3)–(5)) can be used to compare HTFs considering the abovementioned pumping power, fluid volume, and heat losses or temperature drop [13].

$$\text{FOM}_{\text{pumping}} = \frac{\mu^{0.2}}{\rho^2 \cdot C_p^{2.8}} \quad (3)$$

$$\text{FOM}_{\text{volume}} = \frac{\mu^{0.1}}{\rho^{0.84} \cdot C_p^{1.16}} \quad (4)$$

$$\text{FOM}_{\text{heat losses}} = \text{FOM}_{\text{temp drop}} = \frac{\rho^{0.34} \cdot k^{0.6} \cdot C_p^{0.06}}{\mu^{0.44}} \quad (5)$$

The a , b , c , and d sensitivity numbers indicate how much each property affects the FOMs. Higher Mo is preferred for better heat transfer performance, while for better efficiency and economics, lower $\text{FOM}_{\text{pumping}}$ is preferable. Conversely, lower $\text{FOM}_{\text{volume}}$ is preferable to require less coolant volume for the same heat transfer performance under the same pumping power; meanwhile, lower $\text{FOM}_{\text{heat losses}}$ or $\text{FOM}_{\text{temp drop}}$ is preferable because less insulation is required for preventing heat loss.

Considering the abovementioned FOMs, higher density, thermal conductivity, and heat capacity lead to higher heat transfer performance and lower pumping power and coolant volume, but they also increase the heat loss and temperature loss. Conversely, low viscosity improves the heat transfer performance, and reduces pumping power and coolant volume, but worsens the heat loss and temperature drop. When selecting an ATF, which also plays the role of coolant of the EM, not only the abovementioned FOMs are to be considered for the fresh candidate ATF samples, but also the potential evolution of the FOMs over time and at operation temperatures of the EM.

It is very important to study how the changes over time in the composition and degree of oxidation influence the thermophysical properties of ATFs and the impact of these changes on the heat transfer/cooling performance and efficiency of the ATFs. Numerous studies have investigated the changes in viscosity, friction reduction, thermogravimetry, and electrical conductivity of fresh and aged/used ATFs [16–20], but none of these have studied the cooling performance of these ATFs through properties of figures of merit, except

in the case of thermal conductivity. The goal of this work is to study the cooling performance and efficiency of three conventional ATFs, and the influence of their composition and aging on these characteristics. This is not only of interest for the formulation of new ATFs but also to analyse current conventional ATFs used in HEV to determine whether these fluids can efficiently cool the EM when their oxidation increases with use.

2. Materials and Methods

2.1. Automatic Transmission Fluids (ATFs)

Three conventional ATFs (A, B, C) based on mineral oils were selected for this study, and Table 1 portrays the viscosity properties and composition of the ATFs. ATF A was formulated with a mixture of two mineral oils: SP90H and LN-100HS, belonging to API Group I, and composed mainly of iso-paraffins with carbon chain lengths of C16–C30 and C21–C33, respectively. Meanwhile, the ATFs B and C contain a mixture of two mineral oils (YUBASE 3 and YUBASE 6) from API Group III as base fluid, also mainly composed of iso-paraffins with carbon chain lengths of C17–C27 (38.27% for ATF B and 45% for ATF C) and C18–C54 (50.73% for ATF B and 38% for ATF C). The additive packages used in the formulation of these ATFs were: EDR-219 in ATF A, HiTEC 3460 in ATF B, and HiTEC 3488 in ATF C.

Table 1. Composition and viscosity properties of the ATFs.

Properties	ATF A	ATF B	ATF C
Base oils (wt.%)	88.3	89.0	83.0
Additive package (wt.%)	11.7	11	17
Kinematic viscosity (mm ² /s) at 313.15 K (40 °C)	39.4	29.8	36.2
Kinematic viscosity (mm ² /s) at 373.15 K (100 °C)	7.7	5.8	7.4
Viscosity Index	170	144	176

2.2. Ageing Process

Different ageing states of the ATFs were obtained through an artificial oxidation process where the combination of different values of temperature: 423.15 K (150 °C) and 443.15 K (170 °C), air flow (20 and 40 L/h), and time (168 and 216 h) were used. The 8 combinations of the different parameter values were coded from 1 to 8, and the fresh oil sample was coded as 0 (Table 2).

Table 2. Samples used in the different ageing conditions.

Samples	Temp. (K)	Air Flow (L/h)	Time (h)
A0, B0, C0	Fresh oil	Fresh oil	Fresh oil
A1, B1, C1	423.15	20	168
A2, B2, C2	423.15	40	168
A3, B3, C3	443.15	20	168
A4, B4, C4	443.15	40	168
A5, B5, C5	423.15	20	216
A6, B6, C6	423.15	40	216
A7, B7, C7	443.15	20	216
A8, B8, C8	443.15	40	216

2.3. Thermophysical Properties Measurements

The density and the dynamic viscosity of the ATFs (fresh and aged samples) were measured using a Stabinger SVM3001 Viscometer in the temperature range from 298.15 K (25 °C) to 398.15 K (125 °C). The apparatus automatically reports the kinematic viscosity and the viscosity index (VI) values from the density and the dynamic viscosity results.

The thermal conductivity measurements of the ATFs were performed in the temperature range from 288.15 K (15 °C) to 363.15 K (90 °C) with a THW-L2 device (Thermtest Inc., Hanwell, NB, Canada), which uses the transient hot-wire method for measuring thermal

conductivity from 0.01 to 2 W/m·K. A description of the equipment and accessories is presented in [21].

Specific isobaric heat capacity was measured by differential scanning calorimetry (DSC) using a Mettler Toledo DSC 822e with a computer-based controller. A heating ramp from 298.15 K (25 °C) to 398.15 K (125 °C) was used at a heating rate of 5 K/min in an oxygen atmosphere with a flow rate of 50 mL/min. The mass of the sample used in the experiment was 5 mg. Blank experiments were conducted for all experimental protocols (the mass of the sapphire sample reference was 20 mg) and each experiment was repeated three times.

3. Results

The results of the measurements of density, viscosity, thermal conductivity, and heat capacity are portrayed in Figure 2. As expected, density and viscosity showed decreasing values with temperature and the differences among the three ATF s were small. ATF A demonstrated slightly higher density values than ATF s B and C at all temperatures tested. This was also observed for viscosity but only at lower temperatures. Regarding thermal conductivity and heat capacity, the ATF s behaved differently. ATF A demonstrated the lowest thermal conductivity and the highest heat capacity values, whereas ATF C demonstrated the highest thermal conductivity values and similar heat capacity values to ATF B. The differences in the relative values of these properties, despite ATF s B and C being formulated with the same base oils belonging to API Group III, are related to the molecular structure of the distinct hydrocarbon chains of the base oils.

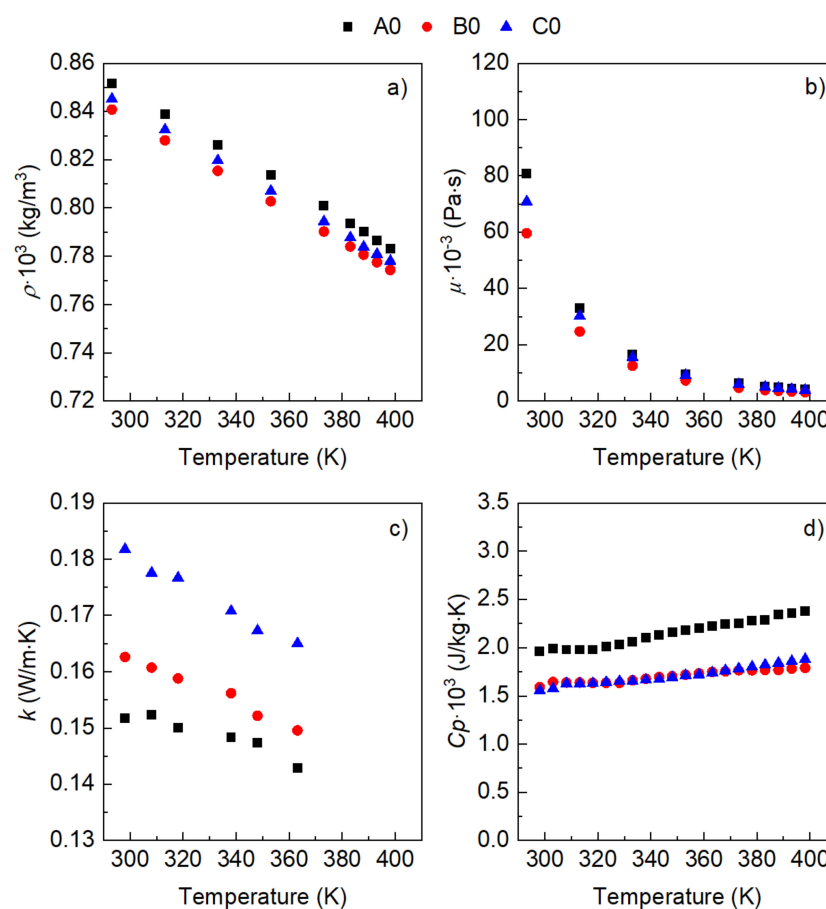


Figure 2. Thermophysical properties of the fresh ATF s (A0, B0, C0): (a) density (ρ), (b) dynamic viscosity (μ), (c) thermal conductivity (k), and (d) heat capacity (C_p).

Unlike electrical conductivity, which is greatly affected by the lubricant additives, thermal properties are closely related to base oil types and molecular structures [19]. In

base oils with a longer main chain, thermal vibration energy is transmitted by intermolecular heat transfer propagated through the main chain and collisions with neighbouring molecules [19,22]. Contrastingly, base oils with a shorter chain and many methyl branches need more intermolecular collisions to transmit thermal vibration energy over the same distance. Narita and Takekawa [22] found a correlation for thermal conductivity and molecular structure (Equation (6)) from the analysis of the quantitative factors structure–property relationship (QSPR) of 74 compounds.

$$\text{Thermal conductivity at } 353.15 \text{ K} = 0.368A - 0.126B + 0.0741C + 0.133D - 0.239 \quad (6)$$

where A is the length of the main chain, B is the number of shorter branches, C is the number of longer branches, and D is the number of aromatic rings. This equation highlights the influence on the thermal conductivity of not only the main chain length and the number of shorter branches but also the number of longer branches and the number of aromatic rings.

Although ATFs B and C are composed of a mixture of the same two base fluids, the concentration of these base oils is different in each ATF and this led to a different concentration of the distinct hydrocarbon chains forming these base fluids, resulting in different thermal conductivities. However, the very similar heat capacity of these two ATFs (B and C) could be related to the presence of an equal number of chemical groups according to the estimation method of heat capacity from group contributions [23].

Figure 3 portrays the figures-of-merit used for the comparison of the cooling performance of the lubricant samples in fresh conditions. Generally, all the lubricant samples have a very similar cooling performance. ATF A0, however, demonstrates lower $FOM_{\text{heat losses}}$ values than the other ATFs, which is advantageous. Conversely, it has a slightly lower Mouromtseff number (M_o).

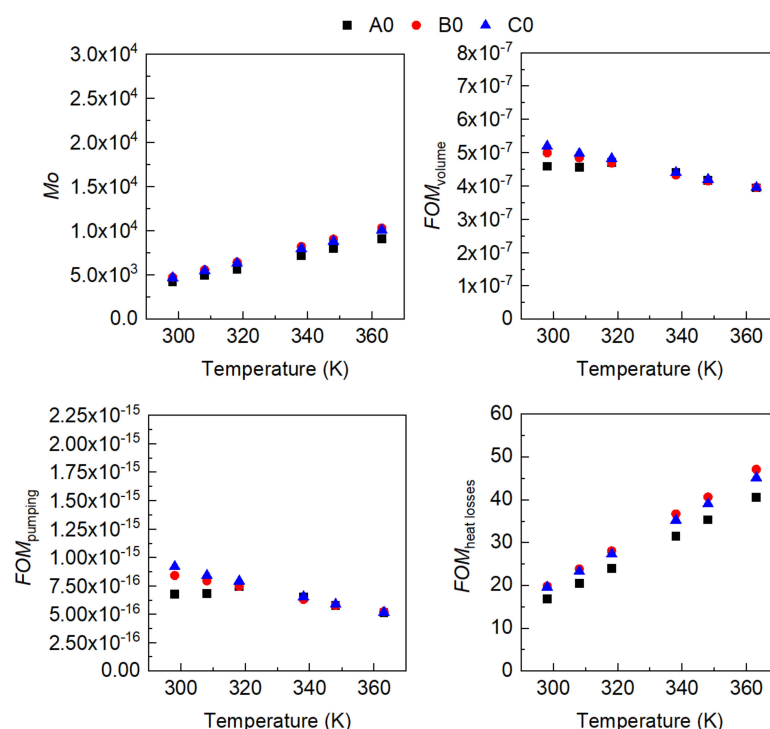


Figure 3. Figures-of-merit (FOM) of the fresh ATFs (A0, B0 and C0).

The oxidation state of the oil samples after the aging process was studied in previous work [20] by using the Fourier transform infrared (FT-IR) spectroscopy technique. The FT-IR spectra obtained from the fresh and aged oil samples demonstrated very slight differences, so the oxidation process was in the “induction phase” according to Besser et al. [24]. However, four clustering zones (Figure 4) were detected after a Principal Component

Analysis of the spectra, demonstrating that similar molecular changes occurred in the ATFs for determined “temperature-air flow-time” combinations coded as 0, 1, 2, 4, 6, and 8 (Table 2). Considering this, a comparison of the thermal behaviour with the degree of oxidation was made by taking the fresh samples (A0, B0, and C0) and their corresponding samples aged under the most severe condition (aging condition coded as 8).

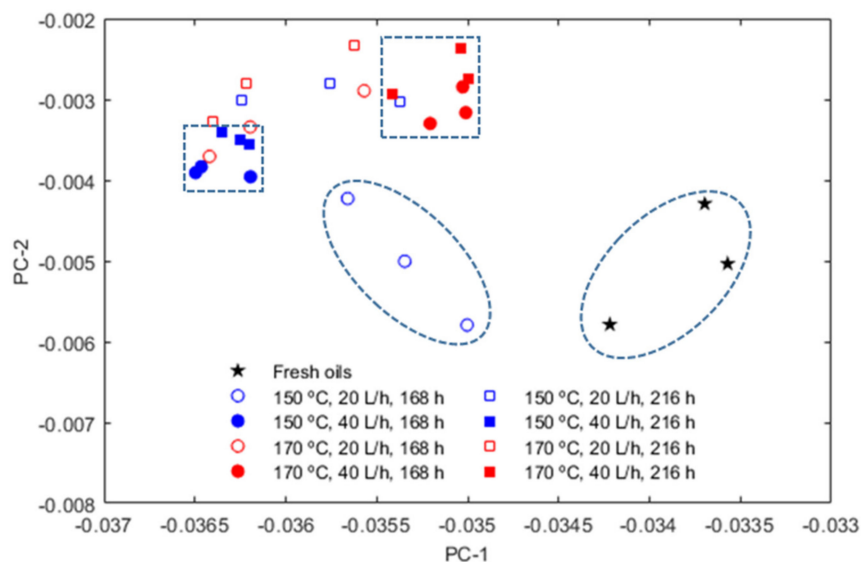


Figure 4. Principal component analysis for all the ATFs from the FTIR spectra [20].

Figure 5 portrays the thermophysical properties of all the ATFs after an artificial oxidation process performed for 216 h at a temperature of 443.15 K (170 °C) and an air flow of 40 L/h. The lubricant samples aged under these conditions are labelled as A8, B8 and C8. The variations in the thermophysical properties of the aged ATFs with temperature were like those of the fresh ATFs, but ATF C demonstrated better performance, with the highest thermal conductivity and intermediate heat capacity values.

The comparison of the thermophysical properties of the fresh ATFs (Figure 2) with those of the aged ATFs (Figure 5) indicates that the aging (oxidation) process of the ATFs led to a slight increase in density and viscosity, while most changes took place in thermal conductivity and heat capacity. The increase in viscosity with oxidation is explained by polymerization reactions, which lead to the formation of high molecular weight products [25], and by the formation of carboxylic acids and ketones, which contribute to the formation of hydrogen bonds and dipole–dipole interaction, resulting in higher intermolecular forces [26]. The thermal conductivity of ATF A increased with aging, while in the case of ATF C, it decreased. Conversely, the thermal conductivity of ATF B remained constant. This behavior could be explained by Equation (1). The oxidation process led to the carbon chains of the branches being shortened preferentially, so the changes in the molecular structure after the oxidation process reduced the number of shorter branches in ATF A and the number of longer branches in ATFs B and C, due to the main constituents of each ATF. However, this effect was lower in ATF B due to the higher percentage of longer chains in this lubricant sample. The reduction in the number of shorter branches in ATF A results in greater thermal vibration energy transferred by intermolecular heat transfer propagated through the main chain, and thus an increase in thermal conductivity was achieved. Contrarily, the reduction in the number of longer branches in ATF C results in the necessity of more intermolecular collisions to transfer thermal vibration energy the same distance and thus the thermal conductivity decreased. Regarding the heat capacity, the increase in this property with oxidation in ATFs B and C and the decrease in ATF A could be explained by the group contributions method reported in [23] but it is out of the scope of this study.

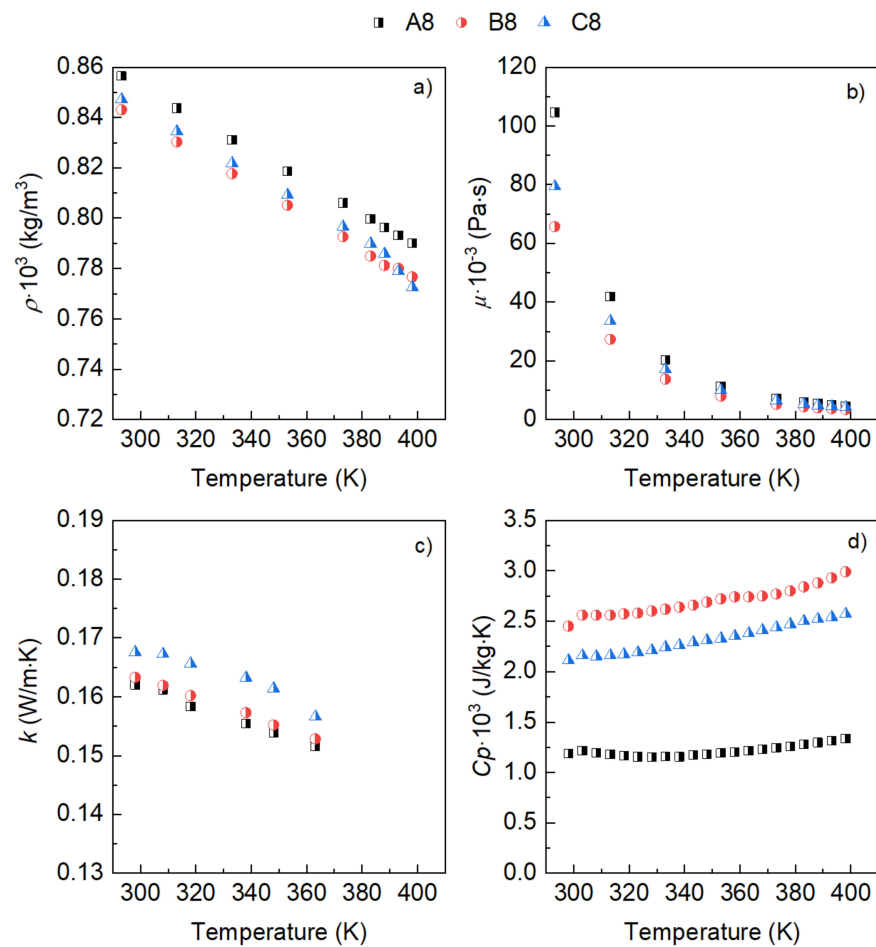


Figure 5. Thermophysical properties of the aged ATFs (A8, B8, C8): (a) density (ρ), (b) dynamic viscosity (μ), (c) thermal conductivity (k), and (d) heat capacity (C_p).

Despite the differences in the measured thermophysical properties of the ATFs after the oxidation process (Figure 5), ATFs B and C demonstrated better cooling performance than ATF A according to their Mouromtseff numbers, $FOM_{pumping}$ and $FOM_{volume \text{ values}}$ (Figure 6). The $FOM_{pumping}$ increased by an order of magnitude for ATF A, while it decreased slightly for ATFs B and C after the oxidation process (aging condition 8).

The oxidation of the ATFs led to different variations in their thermophysical properties, according to the base oils used, according to Figure 5. The variation in these properties with oxidation was determined as $(\theta_{ATF_{aged}} - \theta_{ATF_{fresh}}) / \theta_{ATF_{fresh}}$, where θ is a thermophysical property, and the influence of temperature on each property variation is represented in Figure 7. Whereas density remained constant for all the ATFs, the rest of the thermophysical properties changed with the oxidation process. As expected, the viscosity increased in all the ATFs in the following order: $\mu_{ATF A} > \mu_{ATF B} > \mu_{ATF C}$. Thermal conductivity hardly changed in ATF B, while this property increased for ATF A and decreased for ATF C. Additionally, the heat capacity also demonstrated different behaviors, rising for ATFs B and C, and decreasing for ATF A. The sensitivity to temperature of the variation of these thermophysical properties with oxidation is approximately null, except for the viscosity variation in ATF A, Figure 7.

Figure 8 demonstrates the variation of the FOMs, calculated as $(FOM_{ATF_{aged}} - FOM_{ATF_{fresh}}) / FOM_{ATF_{fresh}}$, with temperature. In this case, ATFs B and C performed very similarly, indicating that cooling performance is mainly determined by the base oils used in the oil formulation. In these two ATFs, the Mouromtseff number increased with oxidation, the FOM_{heat} losses remained constant, and the $FOM_{pumping}$ and the FOM_{volume} decreased. These changes in ATFs B and C make them the best options among the three

studied ATFs. Contrarily, ATF A performed worse with increases in both the $FOM_{pumping}$ and the FOM_{volume} , and a decreasing Mouromtseff number. The sensitivity of the variation of these FOMs to temperature was almost null, except for the $FOM_{pumping}$ of ATF A.

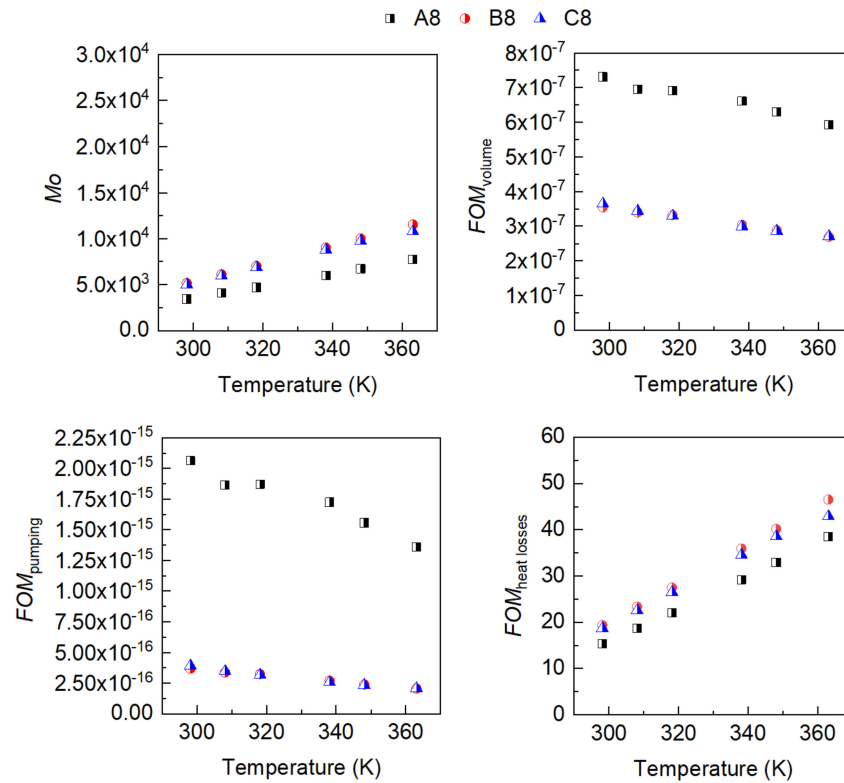


Figure 6. Figures-of-merit (FOMs) of the aged ATFs (A8, B8, C8).

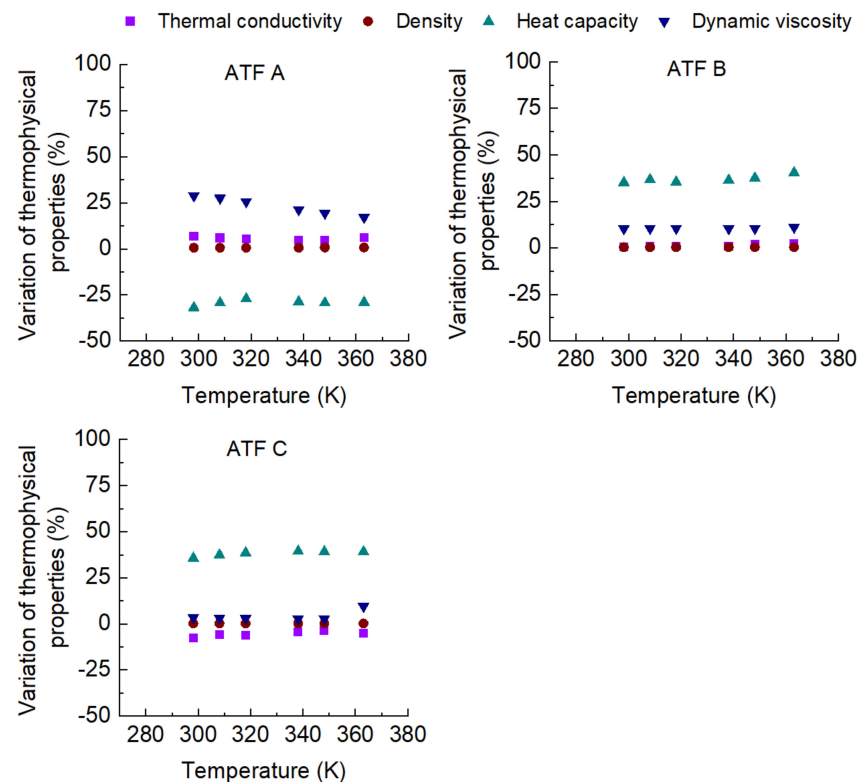


Figure 7. Sensitivity to temperature of the variation of the thermophysical properties with oxidation.

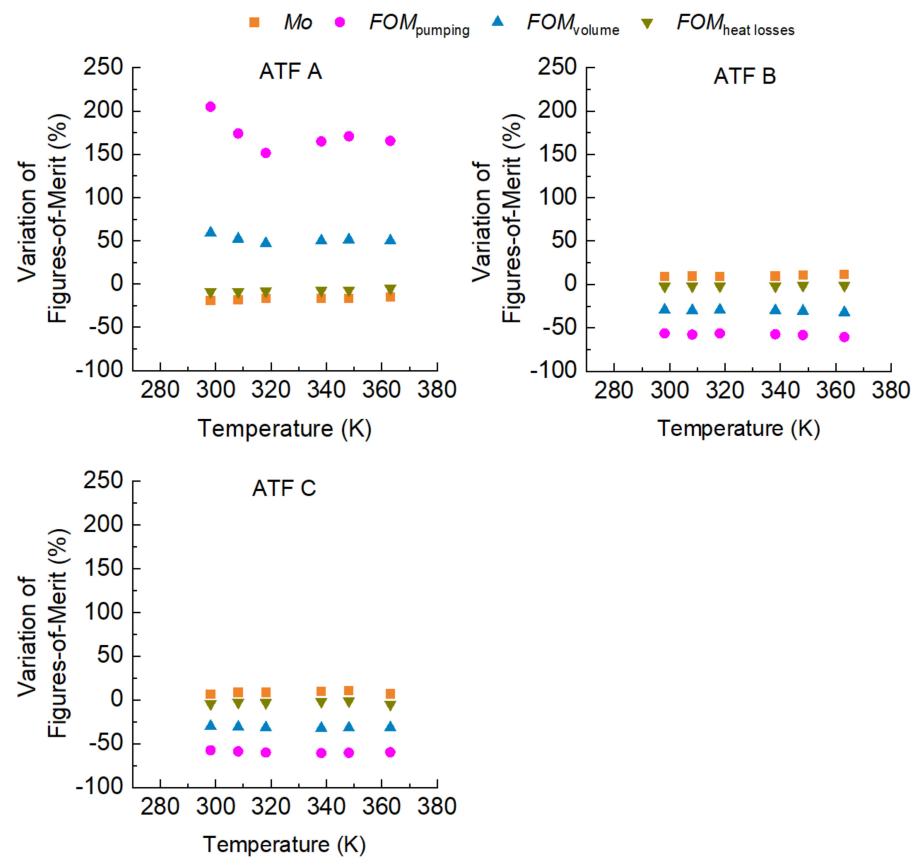


Figure 8. Sensitivity to temperature of the variation of figures-of-merit with oxidation.

4. Conclusions

The ATFs used in EVs, where the EM is located inside the transmission housing, have the role not only of forming a friction- and wear-reduction tribofilm but also protecting against corrosion and removing heat. The lubricants' properties, such as density, viscosity, thermal conductivity, and heat capacity, among others, are important for the heat-transfer rates in many applications, including electric drivetrains. These properties can change with the oxidation of the lubricant that takes place during the use of the ATF and the cooling performance can be seen to be affected. The cooling performance of three conventional ATFs when fresh and aged were studied and the following conclusions could be drawn:

1. The influence of the molecular structure on thermal conductivity and heat capacity is stronger than on density and viscosity, but the differences in these properties of the three conventional ATFs in fresh conditions did not differentiate their cooling performance as expressed through some figures-of-merit (FOMs).
2. The oxidation of the ATFs changed thermal conductivity and heat capacity in a different manner depending on the API Group of the base oils. ATFs B and C, formulated with base oils from API Group III, demonstrated better cooling performance than ATF A, which was formulated with base oils from API Group I.
3. The sensitivity to temperature of the variation with oxidation of the studied properties, including the FOMs, was almost null, except for ATF A.
4. The FOMs should be used to compare cooling performance of ATFs for electric drivetrains instead of a single property such as thermal conductivity.
5. Testing of the cooling performance of ATFs at higher oxidation levels should be addressed in future research.

Author Contributions: Conceptualization, J.L.V. and A.H.B.; methodology, N.R., A.G. and L.L.; investigation, N.R., J.L.V. and J.I.P.; writing—original draft, A.H.B., N.R. and L.L.; supervision, J.L.V.; funding acquisition, A.H.B. and J.L.V.; project administration, A.H.B.; writing—review and editing, A.H.B., J.I.P., L.L. and A.G. All authors have read and agreed to the published version of the manuscript.

Funding: This research was funded by Ministry of Science, Innovation and Universities (Spain) and by the Government of the Principality of Asturias (Spain), grant numbers PID2019-109367RB-I00 and PA-21-AYUD/2021/50987, respectively.

Institutional Review Board Statement: Not applicable.

Informed Consent Statement: Not applicable.

Data Availability Statement: Data is contained within the article.

Acknowledgments: The Scientific-Technical Services of the University of Oviedo are also acknowledged.

Conflicts of Interest: The authors declare no conflict of interest.

Nomenclature

C_p	heat capacity
FOM	figure of merit
k	thermal conductivity
Mo	Mouromtseff number
Greek symbols	
μ	dynamic viscosity
ρ	density

References

- Beyer, M.; Brown, G.; Gahagan, M.; Higuchi, T.; Hunt, G.; Huston, M.; Jayne, D.; McFadden, C.; Newcomb, T.; Patterson, S.; et al. Lubricant Concepts for Electrified Vehicle Transmissions and Axles. *Tribol. Online* **2019**, *14*, 428–437. [CrossRef]
- Farfan-Cabrera, L.I. Tribology of Electric Vehicles: A Review of Critical Components, Current State and Future Improvement Trends. *Tribol. Int.* **2019**, *138*, 473–486. [CrossRef]
- Berly, M. Next Generation Driveline Lubricants for Electrified Vehicles. *Tribol. Lubr. Technol.* **2021**, *77*, 38–40.
- Eckenfels, T.; Kaksa, A.; Marek, C. 48 V Hybridization. *CTI Symp.* **2018**, *2020*, 110–119. [CrossRef]
- Dilzer, M. P2 Hybridization—Tailored Solutions. *CTI Symp.* **2018**, *2020*, 80–86. [CrossRef]
- Toyota Multi-Stage Hybrid System. Available online: <https://global.toyota/en/download/34288283/> (accessed on 18 August 2022).
- Ha, T.; Han, N.G.; Kim, M.S.; Rho, K.H.; Kim, D.K. Experimental Study on Behavior of Coolants, Particularly the Oil-Cooling Method, in Electric Vehicle Motors Using Hairpin Winding. *Energies* **2021**, *14*, 956. [CrossRef]
- Wang, X.; Li, B.; Gerada, D.; Huang, K.; Stone, I.; Worrall, S.; Yan, Y. A Critical Review on Thermal Management Technologies for Motors in Electric Cars. *Appl. Therm. Eng.* **2022**, *201*, 117758. [CrossRef]
- Huang, Z.; Nategh, S.; Lassila, V.; Alakula, M.; Yuan, J. Direct Oil Cooling of Traction Motors in Hybrid Drives. In Proceedings of the 2012 IEEE International Electric Vehicle Conference, IEVC, Greenville, CA, USA, 4–8 March 2012. [CrossRef]
- Huang, Z.; Marquez, F.; Alakula, M.; Yuan, J. Characterization and Application of Forced Cooling Channels for Traction Motors in HEVs. In Proceedings of the 20th International Conference on Electrical Machines, ICEM, Marseille, France, 2–5 September 2012; pp. 1212–1218. [CrossRef]
- Alexandrova, Y.; Semken, R.S.; Pyrhönen, J. Permanent Magnet Synchronous Generator Design Solution for Large Direct-Drive Wind Turbines: Thermal Behavior of the LC DD-PMSG. *Appl. Therm. Eng.* **2014**, *65*, 554–563. [CrossRef]
- Lim, D.H.; Lee, M.Y.; Lee, H.S.; Kim, S.C. Performance Evaluation of an in-Wheel Motor Cooling System in an Electric Vehicle/Hybrid Electric Vehicle. *Energies* **2014**, *7*, 961–971. [CrossRef]
- Kim, E.S.; Sabharwall, P.; Anderson, N. Development of Figure of Merits (FOMs) for Intermediate Coolant Characterization and Selection. In Proceedings of the American Nuclear Society Annual Meeting, Hollywood, FL, USA, 25–30 June 2011.
- Yu, L.; Liu, D. Study of the Thermal Effectiveness of Laminar Forced Convection of Nanofluids for Liquid Cooling Applications. *IEEE Trans. Compon. Packag. Manuf. Technol.* **2013**, *3*, 1693–1704. [CrossRef]
- Mouromtseff, I.E. Water and Forced-Air Cooling of Vacuum Tubes: Nonelectronic Problems in Electronic Tubes. *Proc. IRE* **1942**, *30*, 190–205. [CrossRef]
- Farfan-Cabrera, L.I.; Gallardo-Hernández, E.A.; Vite-Torres, M.; Godínez-Salcedo, J.G. Influence of Oxidation of Automatic Transmission Fluids (ATFs) and Sliding Distance on Friction Coefficients of a Wet Clutch in the Running-in Stage. *Friction* **2021**, *9*, 401–414. [CrossRef]

17. Fatima, N.; Holmgren, A.; Marklund, P.; Minami, I.; Larsson, R. Degradation Mechanism of Automatic Transmission Fluid by Water as a Contaminant. *Proc. Inst. Mech. Eng. Part J J. Eng. Tribol.* **2015**, *229*, 74–85. [[CrossRef](#)]
18. McFadden, C.; Hughes, K.; Raser, L.; Newcomb, T. Electrical Conductivity of New and Used Automatic Transmission Fluids. *SAE Int. J. Fuels Lubr.* **2016**, *9*, 519–526. [[CrossRef](#)]
19. Kwak, Y.; Cleveland, C.; Adhvaryu, A.; Fang, X.; Hurley, S.; Adachi, T. Understanding Base Oils and Lubricants for Electric Drivetrain Applications. *SAE Tech. Pap.* **2019**. [[CrossRef](#)]
20. Rodríguez, E.; Rivera, N.; Fernández-González, A.; Pérez, T.; González, R.; Battez, A.H. Electrical Compatibility of Transmission Fluids in Electric Vehicles. *Tribol. Int.* **2022**, *171*, 107544. [[CrossRef](#)]
21. Prado, J.I.; Calviño, U.; Lugo, L. Experimental Methodology to Determine Thermal Conductivity of Nanofluids by Using a Commercial Transient Hot-Wire Device. *Appl. Sci.* **2021**, *12*, 329. [[CrossRef](#)]
22. Narita, K.; Takekawa, D. Lubricants Technology Applied to Transmissions in Hybrid Electric Vehicles and Electric Vehicles. *SAE Tech. Pap.* **2019**. [[CrossRef](#)]
23. Rihani, D.N.; Doraiswamy, L.K. Estimation of Heat Capacity of Organic Compounds from Group Contributions. *Ind. Eng. Chem. Fundam.* **1965**, *4*, 17–21. [[CrossRef](#)]
24. Besser, C.; Agocs, A.; Ronai, B.; Ristic, A.; Repka, M.; Jankes, E.; McAleese, C.; Dörr, N. Generation of Engine Oils with Defined Degree of Degradation by Means of a Large Scale Artificial Alteration Method. *Tribol. Int.* **2019**, *132*, 39–49. [[CrossRef](#)]
25. El-Naggar, A.Y.; El-Adly, R.A.; Altalhi, T.A.; Alhadhrami, A.; Modather, F.; Ebiad, M.A.; Salem, A. Oxidation Stability of Lubricating Base Oils. *Pet. Sci. Technol.* **2018**, *36*, 179–185. [[CrossRef](#)]
26. Perez, J.M. Oxidative Properties of Lubricants Using Thermal Analysis. *Thermochim. Acta* **2000**, *357*, 47–56. [[CrossRef](#)]